UDK 528.8.044.2:550.34.012:721
Original scientific paper / Izvorni znanstveni članak

Earthquake-Induced Building Recognition Using Correlation Change Detection of Texture Features Based on SAR Data

Qiang LI, Lixia GONG, Jingfa ZHANG – Beijing[1]

ABSTRACT. The detection of building damage due to earthquakes is crucial for disaster management and disaster relief activities. Change detection methodologies using satellite images, such as synthetic aperture radar (SAR) data, have being applied in earthquake damage detection. Information contained within SAR data relating to earthquake damage of buildings can be disturbed easily by other factors. This paper presents a multitemporal change detection approach intended to identify and evaluate information pertaining to earthquake damage by fully exploiting the abundant texture features of SAR imagery. The approach is based on two images, which are constructed through principal components of multiple texture features. An independent principal components analysis technique is used to extract multiple texture feature components. Then, correlation analysis is performed to detect the distribution information of earthquake-damaged buildings. The performance of the technique was evaluated in the town of Jiegu (affected by the 2010 Yushu earthquake) and in the Kathmandu Valley (struck by the 2015 Nepal earthquake) for which the overall accuracy of building detection was 87.8% and 84.6%, respectively. Cross-validation results showed the proposed approach is more sensitive than existing methods to the detection of damaged buildings. Overall, the method is an effective damage detection approach that could support post-earthquake management activities in future events.

Keywords: change detection, synthetic aperture radar, earthquake, correlation analysis, principal component analysis, texture feature.

[1] Qiang Li, Ph.D. candidate, Institute of Engineering Mechanics, China Earthquake Administration, Harbin, CN-150080 Heilongjiang, China; Key Laboratory of Crustal Dynamics, Institute of Crustal Dynamics, China Earthquake Administration, Anning Zhuang Road No. 1, Xisanqi, Haidian District, CN-100085 Beijing, China, e-mail: liqiang08@163.com,

Lixia Gong, Ph.D., Associate Research Fellow, Key Laboratory of Crustal Dynamics, Institute of Crustal Dynamics, China Earthquake Administration, Anning Zhuang Road No. 1, Xisanqi, Haidian District, CN-100085 Beijing, China, e-mail: glx199008@163.com,

Jingfa Zhang, Ph.D., Researcher Fellow, corresponding author, Key Laboratory of Crustal Dynamics, Institute of Crustal Dynamics, China Earthquake Administration, Anning Zhuang Road No. 1, Xisanqi, Haidian District, CN-100085 Beijing, China, e-mail: zhangjingfa08@163.com.

1. Introduction

Earthquakes are sudden natural disasters that can cause considerable loss of human life, widespread damage to buildings and infrastructure, and the occurrence of other natural hazards such as fires, floods, landslides, and debris flows. Among these, the collapse of buildings is generally related to the greatest loss of life and the highest economic cost. Information regarding building damage is essential for rescue, humanitarian, and reconstruction operations in earthquake disaster areas. Optical and synthetic aperture radar (SAR) data have been applied widely in relation to building damage detection (Matsuoka and Yamazaki 2004, Turker and San 2003, Yusuf et al. 2001, Saito et al. 2004, Arciniegas et al. 2007, Gamba et al. 2007, Hoffmann 2007, Chini et al. 2009, Chini et al. 2011, Miura et al. 2013, Ehrlich et al. 2009, Balz and Liao 2010, Brunner et al. 2010, Pan and Tang 2010, Dell'Acqua et al. 2010, Corbane et al. 2011, Tian et al. 2015, Miura et al. 2016). However, availability of optical images cannot be guaranteed because of clouds and atmospheric conditions. Atmospheric effects on SAR data are negligible and thus, the use of SAR backscattering intensity data has shown some successes in the detection of earthquake damage (Bazi et al. 2005, Dong et al. 2011, Trianni and Gamba 2008, Gong et al. 2013, Jin et al. 2012, Liu et al. 2010).

Low- and medium-resolution SAR images can provide a simple, quick, and effective means with which to monitor and evaluate earthquake disasters based on the detection of changes in images obtained before and after an earthquake. If an earthquake causes damage to buildings, there will be a resulting change of the echo signal, which will lead to changes in intensity, coherence, and correlation. Generally, the echo signal from a built-up area is relatively stable. Therefore, if the relevant indicators of an echo signal from a built-up area change, it can be inferred that changes must have occurred to the building structures.

The relationships between the changes of intensity correlation and the interference coherence coefficient with the degree of damage to buildings after the 1995 Kobe earthquake in Japan have been evaluated using ERS-1 SAR imagery (Yonezawa and Takeuchi 2001, Yonezawa et al. 2002). In addition, it was found that the variation of intensity correlation associated with complex coherence was similar. In general, the correlation is arranged according to the size of different object types: urban area > farmland > forest, i.e., the larger the baseline, the poorer the correlation. For urban areas, the damage decorrelation phenomenon is obvious in small baseline data. Decorrelation in SAR imagery can describe the intensity changes attributable to building collapse or damage. The interference is caused by changes in the overall spatial distribution and to the scattering bodies themselves.

Research has shown that a short baseline distance is more conducive to the detection of urban damage. For example, Matsuoka and Yamazaki (2004) combined intensity change information and the coherence coefficient to analyse areas of a city damaged by an earthquake. They proposed a classification index to categorize the degree of earthquake damage to buildings, which was based on a statistical relationship between the image coherence coefficient and the backscatter coefficient difference using ERS-1 SAR imagery. Their technique was demonstrated to achieve good results in a case study of the 1995 Kobe earthquake. Subsequently,

the same authors used ASAR ENVISAT image intensity to detect areas damaged by the 2003 Bam earthquake in Iran (Matsuoka and Yamazaki 2005). The intensity differences and correlation features of SAR images were used to construct a discriminant function to extract the damaged area. This model was later improved and applied to both the 1995 Kobe earthquake and the Peruvian 2007 Pisco earthquake using L-band ALOS PALSAR images. A quantitative description between the SAR image intensity difference and the correlation coefficient and the damage intensity was established using SAR images obtained both before and after the earthquakes, for which the derived results were considered satisfactory (Matsuoka and Nojima 2010).

In SAR data of a city, buildings are often depicted as areas of high brightness. Furthermore, because of the design of roads and the orderly arrangement of houses, buildings also tend to be depicted as neat patterns of high values of greyscale pixels, which constitute obvious texture features. Therefore, SAR images of urban areas have stable textural characteristics with which it is possible to detect changes in the urban environment.

Many parameters are related to the textural characteristics of SAR images and the information regarding change is contained in different channels. Therefore, it is possible that some available information might be lost and erroneous results derived. In view of this problem, this paper proposes a method based on a principal component analysis (PCA) of the texture features to detect correlation change. The method comprises two principal steps. The first step analyses the parameters of the textural characteristics of different buildings with different degrees of earthquake-related damage to obtain the principal components (PCs). The second step calculates the correlation coefficient of the PCs of the previous step and it then extracts earthquake damage information.

The remainder of this paper is organized as follows. Section 2 describes the detail of the method proposed for change detection based on the PCA of texture features. Section 3 introduces the study area and the data sets. Section 4 presents the experimental results, where two data sets are used to demonstrate the effectiveness of the method. Section 5 discusses the extraction accuracy of the different methods and, finally, the conclusions are presented in Section 6.

2. Materials and Methods

Before undertaking feature analysis, SAR images need to be processed by filtering to reduce the influence of speckle noise. Many filtering algorithms are available for this process, such as the Lee filter, Frost filter, enhanced Kuan filter, and Gamma filter. In this study, the Lee filter with a 3×3 window was used. The method proposed in this paper is divided into two main processes: (1) the generation of the PCs of texture features and (2) the automatic analysis of PC correlation. The technical flowchart of the method is shown in Fig. 1.

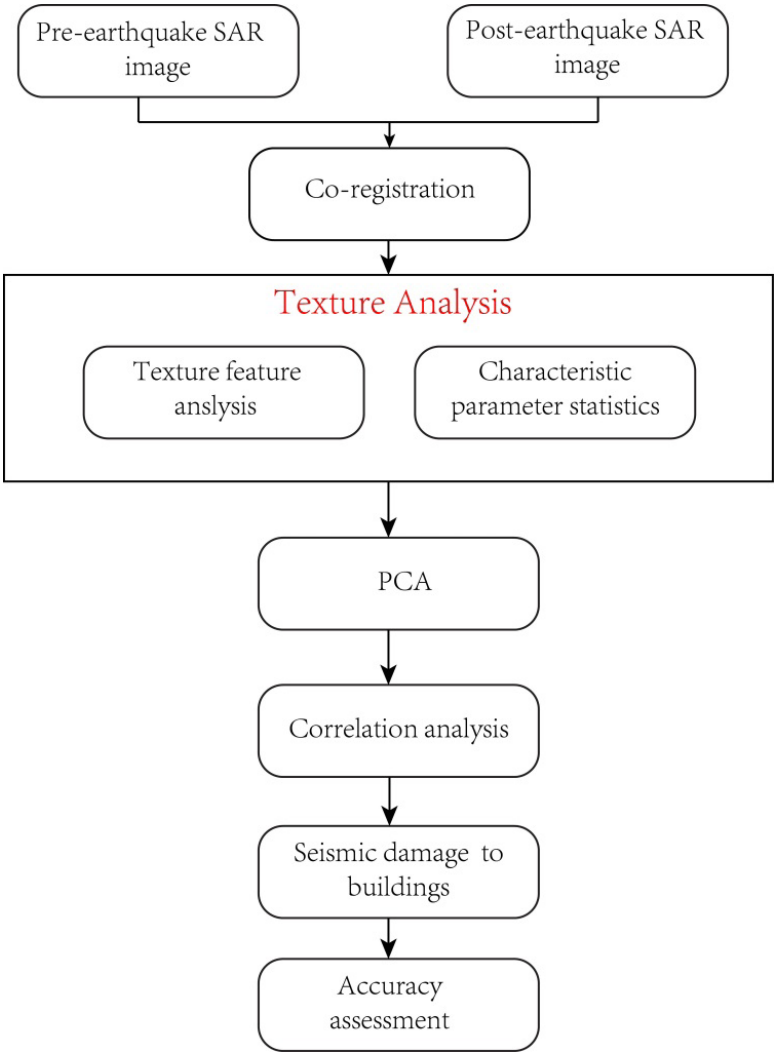

Fig. 1. *Technical flowchart of the proposed correlation change detection method.*

2.1. Generation of optimal texture features

The texture of SAR data mainly reflects the spatial distribution and roughness of the irradiated surface, i.e., the characteristics of the object's surface, which is important for distinguishing surface features (Torres-Torriti and Jouan 2001). Because of the relative lack of spatial information in SAR imagery, the rich textural information is considered the optimal feature in terms of image information recognition and thus, texture analysis of SAR imagery has become increasingly used in a variety of fields.

Different targets have different texture features in SAR images (Manjunath et al. 1996). This means that statistical analysis is an effective method for the interpretation of the texture features of SAR imagery. Statistical analysis methods are mainly used to analyse the texture features within a small area of the image, given the condition that the texture primitives are unknown or have not yet been detected. This is performed mainly to describe the random and spatial statistical characteristics of the texture primitives or local patterns, in order to show consistency within the region and differences between regions. The statistical method plays an important role in texture analysis and it must have good adaptability to the details and randomness of the texture, especially with regard to the complexity of the distribution of natural ground objects. There are many different texture analysis techniques (He et al. 1987, Beliakov et al. 2008, Suyash 2006), e.g., the Linde Buzo Gray, Kekre's Proportionate Error (Kekre et al. 2010), and greyscale-level co-occurrence matrix (GLCM) algorithms. Texture feature extraction based on a co-occurrence matrix of greyscale levels is a classical statistical analysis method that has been applied to the texture extraction of high-resolution and multispectral remote sensing images (Hu et al. 2009).

The co-occurrence probability texture feature uses a GLCM to describe the texture features (Pesaresi and Benediktsson 2001). The GLCM emphasizes the spatial dependence of the greyscale level, which is characterized by the spatial relation of the pixels in a texture pattern (Chen and Deng 2002).The GLCM is a matrix function of pixel distance and angle. It reflects the integrated information of the image in terms of direction, distance, change of amplitude, and speed by calculating the correlation between two points (Clausi and Zhao 2001). Haralick et al. (1973) proposed 14 features based on GLCM for textural analysis. These features measure different aspects of the GLCM and some of the features are correlated. Here, eight texture features are chosen for the analysis: mean (ME), variance (VA), contrast (CON), entropy (ENT), homogeneity (HOM), dissimilarity (DI), correlation (COR), and angular second moment (ASM).

2.1.1. Determination of texture parameters

When textural measures derived from the GLCM are used, some fundamental parameters should be defined, including orientation values, step size, the window size used to calculate the GLCM, and image quantization level.

The arrangement of buildings in an earthquake area is often complex and diverse, which means it is appropriate to take an average value of four directions: 0°, 45°, 90° and 135° as the GLCM of the centre pixel position of the local image. The change of image quantization level has little effect on the GLCM of the image; therefore, a value of 64 is adopted here to calculate the GLCM. Smaller step sizes are better suited to reflect the textural characteristics; here, a step size of 1 is adopted.

The biggest impact on the feature value is the size of the window. Ground investigation can categorize earthquake-related damage to buildings into five categories, whereas remotely sensed earthquake-related damage is divided into three categories: intact buildings, moderately damaged buildings, and destroyed buildings. This paper analyses the parameters of samples in three degrees using different window sizes in order to choose the optimum. Taking variance and entropy as

examples, both quantities are calculated for the change trends of different feature values using window sizes that vary from 3 × 3 to 51 × 51 in intervals of four. Fig. 2 presents the evolution of variance in relation to window size for the textural measures.

The variances of the buildings damaged at different levels reach a maximum for a window size of 11 × 11, following which the variances of the textural features of VA and ENT decrease with larger window sizes. For entropy change, the ability to distinguish between the degrees of intact and moderately damaged buildings is poor, but the results for destroyed buildings are better. The statistical results show an 11 × 11 pixel window to be an appropriate choice for the textural measures.

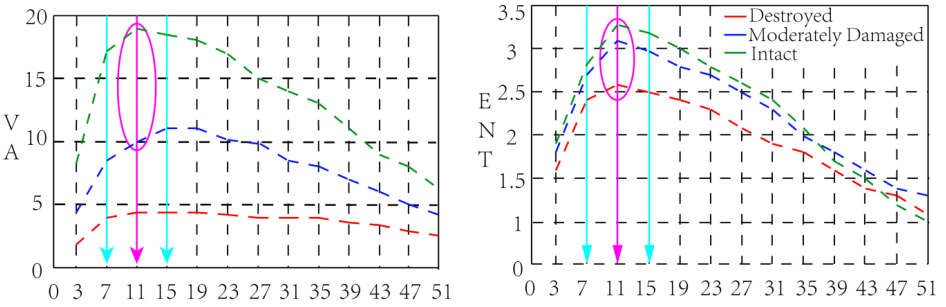

Fig. 2. *Evolution of variance in relation to window size for textural measures.*

2.1.2. Texture feature selection

Multiple texture features have high correlation and feature redundancy. To reduce their inter-correlation, it is necessary to choose optimal texture feature parameters for the statistical analysis. The method of sample statistical analysis is adopted in this experiment. In grouped buildings, the selection of moderately damaged buildings is influenced considerably by humans and the texture feature values of intact and damaged buildings can cover those of moderately damaged buildings. Consequently, intact and destroyed buildings are chosen to participate in this analysis. Samples that were obviously buildings were chosen to determine the statistical characteristics. These samples included 25 intact building samples and 39 destroyed building samples. The texture feature values of the samples are computed separately. To perform the comparative analysis, the parameters are expanded by a factor of 10. Fig. 3 illustrates the statistical analysis of the range of the feature values. The maximum and minimum values of the ME, VA, and HOM parameters are either close or have certain differences between intact and destroyed buildings. There is no intersection between the parameters of the different building categories and therefore, the feature parameters can be used to distinguish buildings with different degrees of damage. In the test area of the SAR image, the ME, VA, and HOM parameters are all capable of characterizing the different degrees of earthquake-related damage of the buildings.

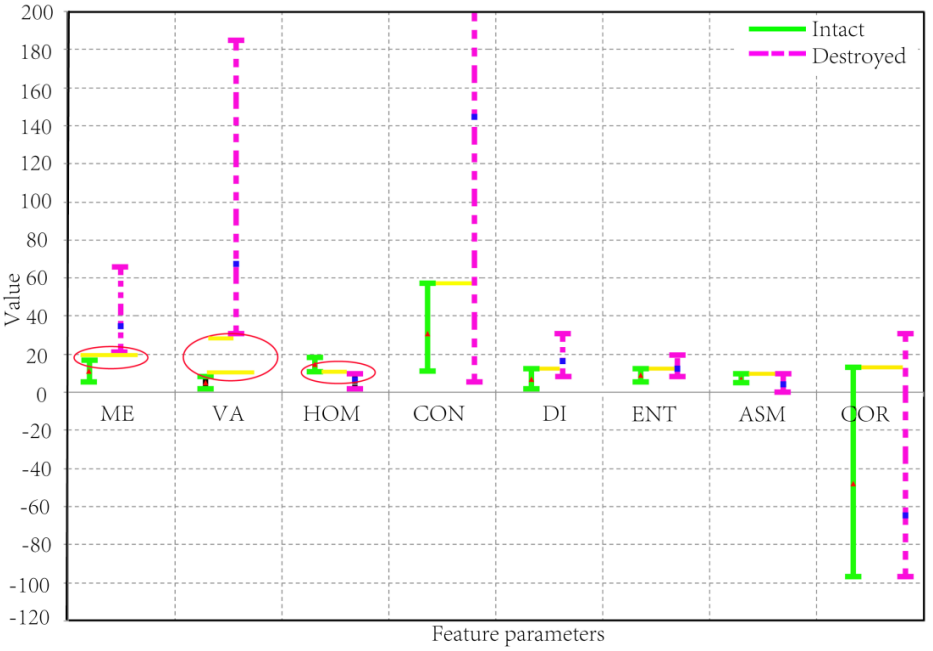

Fig. 3. *Statistical distribution of SAR image characteristic parameters of different types of building. For improved clarity, the scale of the values is enlarged by a factor of 10.*

2.2. PCA

Different features of the data might contain significant correlations, the data set might have few samples and many features (i.e., the data set comprises a small number of samples in high dimensional space), and the data might contain noise. Such problems can lead to an increase in the complexity of the learning algorithm and to a reduction of the generalization ability. PCA is a simple nonparametric method that can overcome these problems to a certain extent, which is why it has been adopted widely in the fields of machine learning and pattern recognition (Baraldi and Parmiggiani 1995, Jolliffe 1986). PCA is able to determine the subspace of a feature vector that causes a data set to be projected onto the subspace (Abdi and Williams 2010); thus, PCA is often used for data compression (Clausen and Wechsler 2000, Sharma et al. 2012). In the field of machine learning, PCs are often considered to contain key features of information data and thus, PCA is often used for feature extraction and dimensionality reduction (Sharma et al. 2012, Martis et al. 2009). In addition, PCA is also often used for signal denoising (Kuncheva and Faithfull 2014).

The greatest advantage of PCA is that there is no parameter setting and optimization requirement in the process of calculation. The central idea of PCA is to reduce the dimensions of the data set as much as possible while preserving its variance. The combination of multiple texture features will have redundant

information in the characterization of the seismic damage of buildings, which will affect the effectiveness of the method to a certain extent. The method of PCA can be used to eliminate the influence of redundant information and to maximize the advantage of the texture features. Since the first PC covers more than 90% of all information, we think the first PC might be appropriate for the analysis and for information detection.

2.3. Correlation change detection

Correlation coefficient analysis is a method based on neighbourhood change detection, which considers adjacent regions rather than isolated pixels; thus, it reduces the influence of noise. The correlation between SAR images at different time phases can be used to determine the differences between the images. Its definition is as follows:

$$r = \frac{\sum_{i=0}^{m,n}(X_{l,s} - \bar{X})(Y_{l,s} - \bar{Y})}{\sqrt{\sum_{i=0}^{m,n}(X_{l,s} - \bar{X})^2} \cdot \sqrt{\sum_{i=0}^{m,n}(Y_{l,s} - \bar{Y})^2}}, \quad (1)$$

where m and N represent the window size; $Y_{l,s}$ and $X_{l,s}$ are the intensity values of the corresponding pixel of the image before and after the earthquake, respectively; and $\bar{Y}$ and $\bar{X}$ represent the average greyscale level of the image before and after the earthquake, respectively. The range of the correlation coefficient r is $[-1, 1]$ and the absolute value of r is close to 1. The closer the linear relationship between the two images, the higher the degree of similarity. In this experiment, the correlation analysis calculation window size is taken as 3 and the correlation coefficient r adopts the absolute value; therefore, its value range is [0, 1].

3. Case study and data sets

The investigated case studies are the earthquakes that struck Yushu County on 14 April 2010 (Mw 7.1) and Nepal on 25 April 2015 (Mw 7.0). This analysis is based on several images, as shown in Table 1. The epicentre of the Yushu earthquake was located near the town of Jiegu in Yushu County (Qinghai Province, China) and the epicentral intensity was 9 degrees. This earthquake affected an area of about 30,000 m^2, causing more than 2000 deaths and huge economic losses (Yu 2010, Li et al. 2013). The main sensor for detecting Yushu earthquake damage is the ALOS PALSAR, which is operated by the Japan Aerospace Exploration Agency. It operates in the L-band, which allows higher coherence over longer periods compared with SAR sensors using the X- or C-bands. This sensor provides high-resolution data because of its very accurate orbital control and its revisit frequency is adequate for meeting the requirements of land and disaster monitoring.

Following the Nepal earthquake, 67,871 fully damaged buildings and 73,624 partially damaged buildings were reported in the Kathmandu Valley. The main data used in the analysis comprise two multitemporal SAR images acquired on 20 April

and 28 April 2015 by the Sentinel-1 satellite, which is operated by the European Space Agency. The spatial resolution of the images is 12 m. Details of the times of data acquisition and image resolution are presented in Table 1. The two data sets are shown in Fig. 4.

Table 1. *Satellite images used in this study.*

Area	Satellite images	Acquisition date	Spatial resolution (m)
The town of Jiegu in Yushu earthquake	ALOS-PALSAR	2010/01/15	16
	ALOS-PALSAR	2010/04/17	16
Kathmandu Valley in Nepal earthquake	Sentinel-1	2015/4/20	12
	Sentinel-1	2015/4/28	12

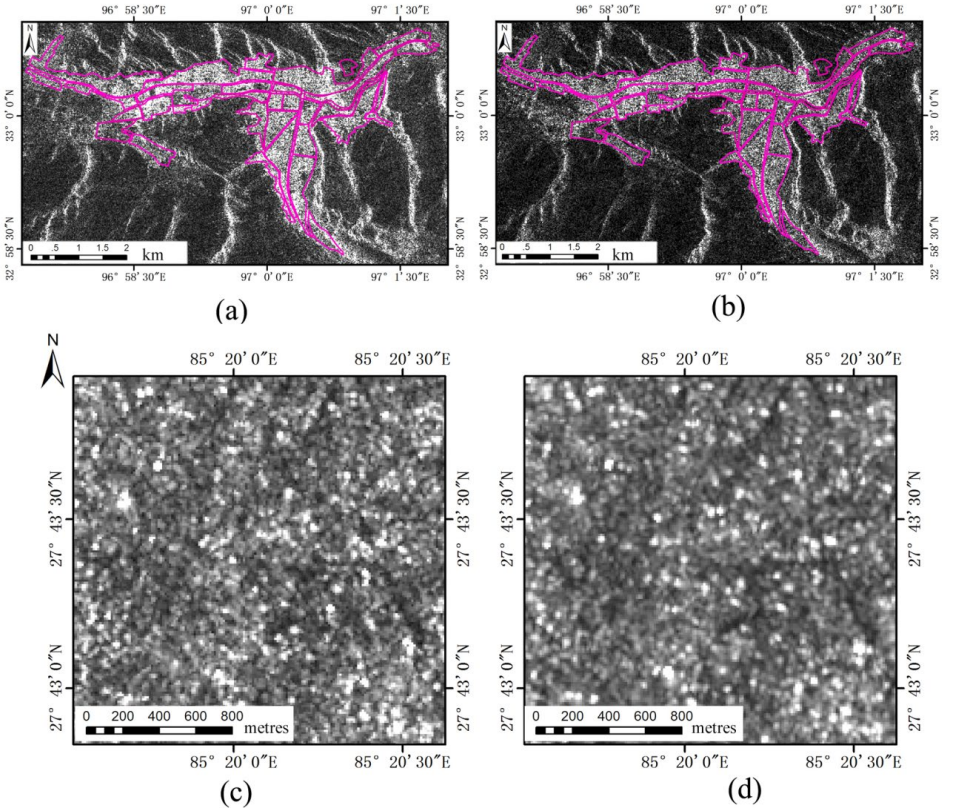

Fig. 4. *Multitemporal SAR images of the Yushu and Nepal earthquake zones: (a) and (b) ALOS SAR images before and after the Yushu earthquake, respectively and (c) and (d) Sentinel-1 SAR images before and after the Nepal earthquake, respectively.*

4. Results

In this section, the experimental results of different algorithms are presented. Furthermore, the parameter setting used in our experiment is given. Prior to analysis, the images were registered using the ENVI software automatic registration algorithm. To obtain texture features, several parameters must be chosen. In the step of deriving the GLCM, the window size is set to 11 × 11. In the step of the PCA, the first PC is adopted to obtain the results. The window size of the correlation calculation is 3 × 3. In the correlation threshold classification, Gong and Zhang (2013) summarized the relationship between the correlation threshold and damage to buildings using ALOS data for the Dujiangyan area (Fig. 5) and we refer to these threshold parameters to obtain our results.

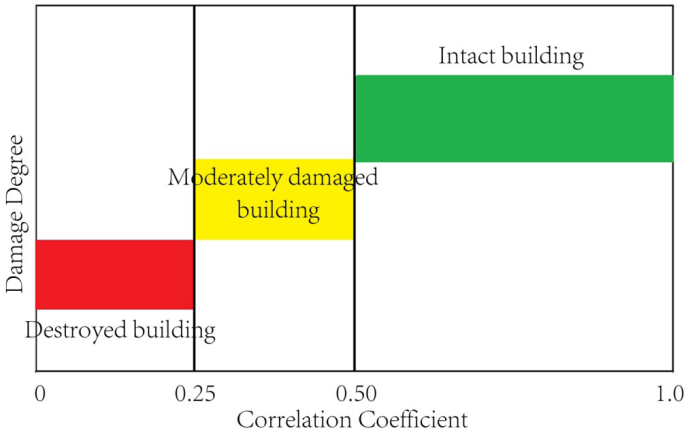

Fig. 5. *Statistical distribution of SAR image characteristic parameters of different types of building.*

To verify the feasibility and accuracy of our proposed method, we display the numerical results using two different data sets. All experiments aimed to verify the following points: (1) to demonstrate that the proposed PC texture feature correlation (TFC) could provide better performance compared with original intensity correlation (OTC) and TFC and (2) to show that change detection based on PCA of texture has greater accuracy compared with traditional texture methods. With regard to the first point, three change detection methods are compared to verify the effectiveness of PCTFC. To address the second point, the PCA of texture is compared against a single texture used in the change detection method under the same situation.

4.1. Change detection based on principal component texture feature correlation

Based on image filtering, the texture feature value was calculated using the GLCM method and the values of the three characteristic parameters (ME, CV, and HOM) were extracted. Fig. 6 presents the first PC of the texture features of ME, CV, and HOM before and after the earthquake. The correlation between the PCs was calculated in conjunction with field survey data (i.e., damage to each building).

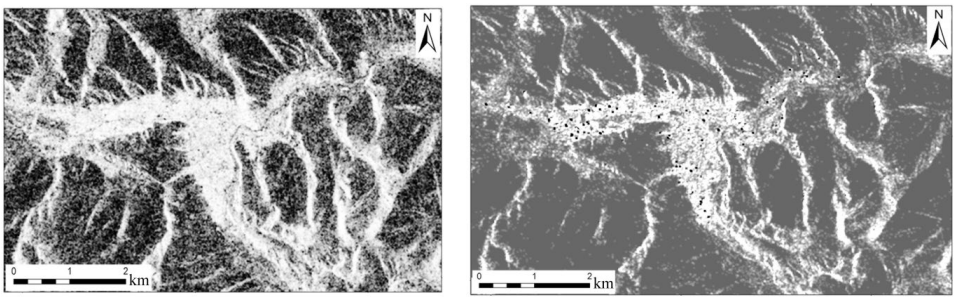

Fig. 6. *First PC of texture features of ME, CV, and HOM: (a) before and (b) after the Yushu earthquake.*

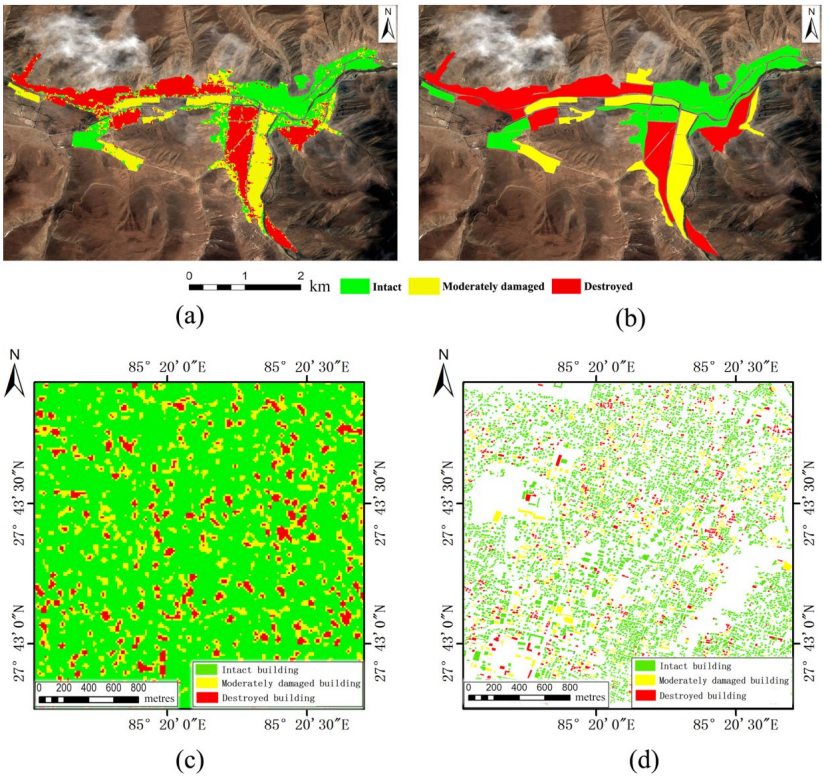

Fig. 7. *Distribution of earthquake damage using the proposed method. (a) Distribution map of building damage caused by the Yushu earthquake. The extraction results are masked by building area. The base image map is a QuickBird image. (b) Result of comparison of the Yushu earthquake. (c) Distribution map of building damage caused by the Nepal earthquake. The discrete pixels in the result are processed by merging. (d) Result of visual interpretation of an optical image. The image for visual interpretation was a GaoFen-2 (GF-2) image. The unit of interpretation is a single building. For details on the standard of interpretation, see the main text.*

We selected an empirical threshold to segment the correlation coefficient and then merged the discrete pixels. Fig. 7(a) illustrates the distribution map of damage caused by the Yushu earthquake and Fig. 7(b) presents results for comparison (Guo et al. 2010). Fig. 7(c) illustrates the distribution map of damage caused by the Nepal earthquake. Because of the lack of field survey data in relation to the Nepal earthquake, we obtained the building distribution map by careful interpretation of a GF-2 post-earthquake optical image for our analysis. The results of the interpretation are shown in Fig. 7(d).

4.2. Change detection based on the original intensity correlation

To compare the characterization ability of texture features, SAR intensity data were used for reference. The intensity image was used directly for the correlation analysis to obtain the distribution of the buildings based on image pre-processing. Fig. 8(a) and 8(b) presents the distribution map of the earthquake damage results for Jiegu and Kathmandu Valley, respectively.

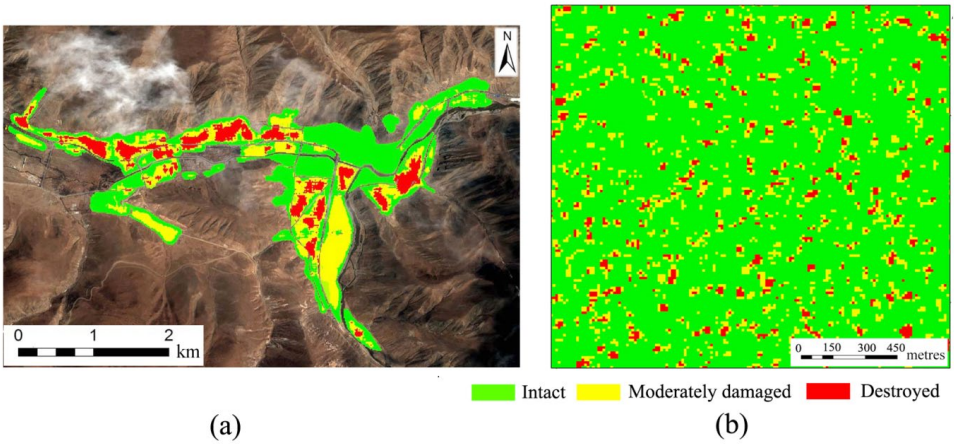

Fig. 8. *Distribution of the OTC results of earthquake damage. (a) Distribution of the OTC results of Yushu earthquake damage. The base image map is a QuickBird image. The discrete pixels in the result are processed by merging. (b) Distribution of the OTC results of Nepal earthquake damage. The discrete pixels in the result are processed by merging.*

4.3. Change detection based on texture feature correlation

To compare the difference between multiple and single texture features, we select the single texture feature of the HOM parameter to compare the results. HOM is a measure of the local greyscale homogeneity of an image. The HOM feature parameter was chosen as the variable for calculating the correlation using the same window size and the distribution of the buildings was analysed. Fig. 9(a) and 9(b) presents the distribution map of the earthquake damage results for Jiegu and Kathmandu Valley, respectively, using the HOM feature correlation change detection.

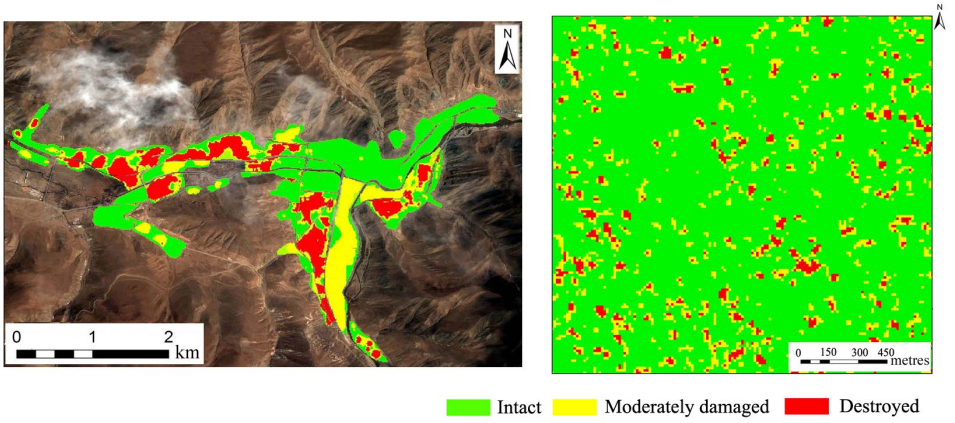

Fig. 9. *Distribution of the TFC results of earthquake damage. (a) Distribution of the TFC results of Yushu earthquake damage. The base image map is a QuickBird image. The discrete pixels in the result are processed by merging. (b) Distribution of the TFC results of Nepal earthquake damage. The discrete pixels in the result are processed by merging.*

5. Discussion

Following the performance outlined in the previous sections, the performance of PCTFC was compared with OTC and TFC quantitatively using prepared interpretation images. In addition to visual inspection, four quantitative measures for evaluating the change detection results were used to assess the quality of the information detected. The quantitative analysis of the change detection results included extraction accuracy (EA), missed rate (MR), false detection rate (FDR), and overall accuracy (OA), which are calculated as follows:

$$EA = {(ea - fa)}/{Ta}, \tag{2}$$

$$MR = {ma}/{Ta}, \tag{3}$$

$$FDR = {fa}/{Ta}, \tag{4}$$

where ea is the extraction area, fa is the false detection area, ma is the missing area, and Ta is the field survey area. The calculation method for OA is the same as for EA and it expresses the overall accuracy of the three types of buildings with different degrees of damage.

The accuracy parameters of the PCTFC method are presented in Tables 2 and 3. The tables also compare the proposed PCTFC accuracy with respect to using

various features. Table 2 presents the performances of the different methods for the case of the Yushu earthquake using ALOS SAR data. For this data set, PCTFC had greater OA compared with OTC and TFC. Furthermore, the EA of moderately damaged and destroyed buildings extracted by PCTFC was the highest.

Table 2. *Accuracy measures for the Yushu earthquake. For details on the accuracy measures (EA, MR, FDR), see the main text.*

Method	Intact building			Moderately damaged building			Destroyed building			OA(%)
	EA(%)	MR(%)	FDR(%)	EA(%)	MR(%)	FDR(%)	EA(%)	MR(%)	FDR(%)	
PCTFC	88.7	11.3	9.4	86.4	13.6	12.1	84.8	15.2	11.7	87.8
OTC	86.2	13.8	17.2	66.7	33.3	30.8	60.5	39.5	10.1	68.9
TFC	89.6	10.4	21.9	74.4	25.6	18.7	63.9	36.1	6.7	76.2

Table 2 shows that the EA of PCTFC for the three categories of damage to buildings was about 85% and the FDR was about 10%. Image analysis showed that the section of detection error was distributed mainly along the roads. This is attributable to the selected correlation window size, whereby road information is incorporated in the calculation causing partial false detection.

The OA of building extraction based on OTC was 68.9%. The EA of moderately damaged buildings was 66% but the FDR was relatively high. Comparison with the results of visual interpretation indicated that some moderately damaged buildings were wrongly classified as intact, especially in built-up areas near roads. Again, this error could be attributed to the influence of roads. The EA of damaged buildings by OTC was about 60%. This is because some peripheral parts of some destroyed buildings were missed or were wrongly classified.

The OA value based on TFC was 76.2%. The EA of intact buildings was high (close to 90%), whereas for destroyed buildings, it was about 64%, although the FDR was low. Some intact buildings were classified as damaged and some moderately damaged or destroyed buildings were classified as intact. Compared with PCTFC, the EA was low. This is because the PCTFC method combines the characteristics of multiple texture parameters that reflect damage information more accurately and it avoids false detection and misses.

Table 3 presents the performances of the different methods using Sentinel-1 SAR data. First, it can be seen that the PCTFC method had higher OA. Moreover, its EAs of the three damage degrees were better than the other two methods (>80%) and it had lower FDRs. This means that PCA of texture features provides the primary contribution for this data set. Second, the MR and FDR of PCTFC were both lower than OTC and TFC for moderately damaged and destroyed buildings, demonstrating the method has greater ability to detect slight changes. Third, the EA of the OTC method was clearly lower than the other methods, while the MR (about 30%) and FDR (>16%) were the highest. This shows that texture features can play an important role in the recognition of seismic damage to buildings.

The seismic damage identification maps produced by these methods are illustrated in Section 3. From Fig. 7(c), it can be seen that the PCTFC method has great ability to resist the effects of noise. Fig. 8(b) shows that traditional OTC methods might cause distortion. Thus, it is evident that the combination of PCA and texture features provided the best recognition results.

Table 3. *Accuracy measures for the Nepal earthquake. For details on the accuracy measures (EA, MR, FDR), see the main text.*

Method	Intact building			Moderately damaged building			Destroyed building			OA(%)
	EA(%)	MR(%)	FDR(%)	EA(%)	MR(%)	FDR(%)	EA(%)	MR(%)	FDR(%)	
PCTFC	82.1	17.9	22.8	84.3	15.7	9.6	86.9	13.1	10.5	84.6
OTC	69.4	30.6	28.5	66.8	33.2	19.7	65.4	34.6	16.8	65.3
TFC	82.4	17.6	24.0	75.2	24.8	15.6	76.5	23.5	22.9	79.4

6. Conclusions

In this paper, a novel extraction method based on the PC correlation of multiple texture features, specifically oriented toward the analysis of multitemporal SAR images of earthquakes, was presented. The approach combined texture features with multiple characteristic parameters. It obtained the most abundant component of earthquake damage using a PC transformation, following which a correlation analysis was performed. ALOS data of the 2010 Yushu earthquake and Sentinel-1 data of the 2015 Nepal earthquake were used as case studies, which demonstrated that the change detection method based on PC correlation has greater detection accuracy than original change detection methods based on intensity image correlation.

Two novel methodological contributions distinguish this work from traditional techniques for the extraction of buildings from SAR images: (1) the combination of PCA and correlation analysis breaks the traditional method of direct change detection based on texture features and (2) the information of earthquake-damaged buildings is extracted based on the form of the PC and multiple texture features. Traditional change detection methods based on texture features usually use the texture feature as the variable and the difference method is used to detect the change information directly. Here, the texture feature was used as the variable of the correlation analysis. The correlation between the two was calculated and the difference from the intensity map caused by other interference factors was avoided. Traditional change detection methods based on texture features are aimed only at a single characteristic parameter, for which information might be limited. Thus, further features could be obtained based on this method in future research. Because of the second contribution above, PCA was performed by fusing multiple texture feature parameters to obtain the information-rich component. This avoided the loss of valuable information and it improved the accuracy of identification.

The case studies of the Yushu and Nepal earthquakes proved the effectiveness of the proposed method. Experimental results showed that the ME, VA, and HOM parameters could effectively characterize the different degrees of earthquake-related building damage and the correlation analysis of three of the PCs could effectively improve the accuracy of identification. As expected, the combination of PCA and texture features provided better performance and led to higher recognition accuracy. In future work, it will be possible to select the detailed results of the investigation of single buildings using field survey data for validation.

ACKNOWLEDGMENTS. The authors wish to thank the anonymous reviewers for their valuable comments. This work was supported by the National Natural Science Foundation of China (Grant No. 41374050), the Special Item for Public Welfare of Scientific Research Project from Institute of Crustal Dynamics, China Earthquake Administration (Grant No. ZDJ-2017-29) and Civil Aerospace Project (Grant No. D010102).

AUTHOR CONTRIBUTIONS. Jingfa Zhang and Qiang Li conceived and designed the experiments; Qiang Li performed the experiments; Jingfa Zhang and Lixia Gong analyzed the data; Qiang Li and Lixia Gong wrote the paper.

CONFLICTS OF INTEREST. The authors declare there are no conflicts of interest regarding the publication of this paper.

References

Abdi, H., Williams, L. J. (2010): Principal Component Analysis, Wiley Interdisciplinary Reviews Computational Statistics, 2(4), 433–459.

Arciniegas, G. A., Bijker, W., Kerle, N., Tolpekin, V. A. (2007): Coherence- and Amplitude-Based Analysis of Seismogenic Damage in Bam, Iran, Using Envisat ASAR Data, IEEE Trans. Geosci. Remote Sens, 45, 1571–1581.

Balz, T., Liao, M. (2010): Building-damage detection using post-seismic high-resolution SAR satellite data, Int. J. Remote Sens, 31, 3369–3391.

Baraldi, A., Parmiggiani, F. (1995): An investigation of the textural characteristics associated with gray level co-occurrence matrix statistical parameters, IEEE Transactions on Geoscience and Remote Sensing, 33(2), 293–304.

Bazi, Y., Bruzzone, L., Melgani, F. (2005): An unsupervised approach based on the generalized Gaussian model to automatic change detection in multitemporal SAR images, IEEE Trans. Geosci. Remote Sens, 43, 874–887.

Beliakov, G., James, S., Troiano, L. (2008): Texture recognition by using GLCM and various aggregation functions, In 2008 IEEE International Conference on Fuzzy Systems: proceedings FUZZ-IEEE 2008, IEEE, Piscataway, N. J.

Brunner, D., Lemoine, G., Bruzzone, L. (2010): Earthquake Damage Assessment of Buildings Using VHR Optical and SAR Imagery, IEEE Trans. Geosci. Remote Sens, 48, 2403–2420.

Chen, Z. P., Deng, P. (2002): Application of textural features to change detection in SAR Image, Remote Sensing Technology and Application, 17(3), 162–166.

Chini, M., Pierdicca, N., Emery, W. J. (2009): Exploiting SAR and VHR Optical Images to Quantify Damage Caused by the 2003 Bam Earthquake, IEEE Trans. Geosci. Remote Sens, 47, 145–152.

Chini, M., Cinti, F. R., Stramondo, S. (2011): Co-seismic surface effects from very high resolution panchromatic images: the case of the 2005 Kashmir (Pakistan) earthquake, Nat. Hazards Earth Syst, 11, 931–943.

Clausen, C., Wechsler, H. (2000): Color image compression using pea and back propagation learning, Pattern Recognition, 33(9), 1555–1560.

Clausi, D., Zhao, Y. (2001): Rapid determination of co-occurrence texture features, Geoscience and Remote Sensing Symposium, IEEE 2001 International.

Corbane, C., Saito, K., Dell'Oro, L., Bjorgo, E., Gill, S. P. D., Emmanuel Piard, B., et al. (2011): A Comprehensive Analysis of Building Damage in the 12 January 2010 Mw7 Haiti Earthquake Using High-Resolution Satellite and Aerial Imagery, Photogramm. Eng. Remote Sens, 77, 997–1009.

Dell'Acqua, F., Bignami, C., Chini, M., Lisini, G., Polli, D. A., Stramondo, S. (2010): Earthquake Damages Rapid Mapping by Satellite Remote Sensing Data: L'Aquila April 6th, 2009 Event, IEEE J. Sel. Top. Appl. Earth Obs. Remote Sens, 4, 935–943.

Dong, Y., Li, Q., Dou, A., Wang, X. (2011): Extracting damage caused by the 2008 Ms8.0 Wenchuan earthquake from SAR remote sensing data, J. Asian Earth Sci, 40, 907–914.

Ehrlich, D., Guo, H. D., Molch, K., Ma, J. W., Pesaresi, M. (2009): Identifying damage caused by the 2008 Wenchuan earthquake from VHR remote sensing data, Int. J. Digit. Earth, 2, 309–326.

Gamba, P., Dell'Acqua, F., Trianni, G. (2007): Rapid Damage Detection in the Bam Area Using Multitemporal SAR and Exploiting Ancillary Data, IEEE Trans. Geosci. Remote Sens, 45, 1582–1589.

Gong, L. X., Zhang, J. F. (2013): Seismic damage building extraction based on correlation change detection, China, Seismological Society Space on Earth Observation Specialized Committee 2013 Academic Seminar, 23.

Gong, L. X., Zhang, F. J., Zeng, Q. M. (2013): A survey of earthquake damage detection and assessment of buildings using SAR, Journal of Earthquake Engineering and Engineering Vibration, 33(4), 195–201.

Guo, H. D., Bing, Z., Lei, L. P., Li, Z., Yu, C. (2010): Spatial distribution and inducement of collapsed buildings in Yushu earthquake based on remote sensing analysis, Science China Earth Science, 53(6), 794–796.

Haralick, R. M., Shanmugan, K., Dinstein, I. (1973): Texture features for image classification, IEEE Transactions on System, Man and Cybernetics, 3, 610–621.

He, D. C., Wang, L., Guibert, J. (1987): Texture feature extraction, Pattern Recognition Letters, 6(4), 269–273.

Hoffmann, J. (2007): Mapping damage during the Bam (Iran) earthquake using interferometric coherence, Int. J. Remote Sens, 28, 1199–1216.

Hu, Z. L., Li, H. Q., Du, P. J. (2009): Study on the extraction of texture features and its application in classifying SAR images, Journal of China University of Mining & Technology, 38(3), 422–427.

Jin, D. J., Wang, X. Q., Dou, A. X. (2012): Review on the methods of earthquake-induced building damage information extraction from SAR images, Remote Sensing Technology and Application, 27(3), 449–457.

Jolliffe, I. T. (1986): Principal Component Analysis, Springer, 14(27), 231–246.

Kekre, H. B., Thepade, S. D., Sarode, T. K. (2010): Image retrieval using texture features extracted from GLCM, LBG and KPE, International Journal of Computer Theory and Engineering, 5(2), 1793–8201, 695–700.

Kuncheva, L. I., Faithfull, W. J. (2014): Pea feature extraction for change detection in multidimensional unlabeled data, Neural Networks and Learning Systems, 25(1), 69–80.

Li, J. W., Bo, J. S., Lu, T. (2013): Seismic damage analysis of school buildings in Yushu Ms7.1 earthquake, Journal of Natural Disasters, 1(22), 123–129.

Liu, Y. H., Qu, C. Y., Shan, X. J. (2010): Application of SAR data to damage identification of the Wenchuan Earthquake, Acta Seismoligica Sinica, 32(2), 214–223.

Manjunath, B. S., Ma, W. Y. (1996): Texture features for browsing and retrieval of image data, IEEE Transactions on Pattern Analysis and Machine Intelligence, 18, 837–842.

Martis, R. J., Chakraborty, C., Ray, A. K. (2009): An integrated ecg feature extraction scheme using pea and wavelet transform, India Conference (INDICON) Annual IEEE.IEEE, 1–4.

Matsuoka, M., Nojima, N. (2010): Building damage estimation by integration of seismic intensity information and satellite L-band SAR imagery, Remote Sensing, 2(9), 2111–2126.

Matsuoka, M., Yamazaki, F. (2004): Use of Satellite SAR Intensity Imagery for Detecting Building Areas Damaged Due to Earthquakes, Earthq. Spectra, 20, 975–994.

Matsuoka, M., Yamazaki, F. (2005): Building damage mapping of the 2003 Bam, Iran, earthquake using ENVISAT/ASAR intensity imagery, Earthquake Spectra, 21(S1), 285–294.

Miura, H., Midorikawa, S., Kerle, N. (2013): Detection of Building Damage Areas of the 2006 Central Java, Indonesia, Earthquake through Digital Analysis of Optical Satellite Images, Earthq. Spectra, 29, 453–473.

Miura, H., Midorikawa, S., Matsuoka, M. (2016): Building Damage Assessment Using High-Resolution Satellite SAR Images of the 2010 Haiti Earthquake, Earthq. Spectra, 32, 591–610.

Pan, G., Tang, D. (2010): Damage information derived from multi-sensor data of the Wenchuan Earthquake of May 2008, Int. J. Remote Sens, 31, 3509–3519.

Pesaresi, M., Benediktsson, J. A. (2001): A new approach for the morphological segmentation of high-resolution satellite imagery, IEEE Transactions on Geoscience and Remote Sensing, 39(2), 309–320.

Saito, K., Spence, R. J. S., Going, C., Markus, M. (2004): Using High-Resolution Satellite Images for Post-Earthquake Building Damage Assessment: A Study Following the 26 January 2001 Gujarat Earthquake, Earthq. Spectra, 20, 145–169.

Sharma, L. N., Dandapat, S., Mahanta, A. (2012): Multichannel ecg data compression based on multiscale principal component analysis, Information Technology in Biomedicine, 16(4), 730–736.

Suyash, P. (2006): Unsupervised texture segmentation with nonparametric neighborhood statistics, ECCV, 2, 494–507.

Tian, A. J., Nielsen, A., Reinartz, P. (2015): Building damage assessment after the earthquake in Haiti using two post-event satellite stereo imagery and DSMs, Int. J. Image Data Fusion, 6, 155–169.

Torres-Torriti, M., Jouan, A. (2001): Gabor vs. GMRF features for SAR imagery classification, Image Processing, In: Proceedings 2001 International conference on IEEE, 1043–1046.

Trianni, G., Gamba, P. (2008): Damage detection from SAR imagery: Application to the 2003 Algeria and 2007 Peru earthquakes, Int. J. Navig. Obs, 1–8.

Turker, M., San, B. T. (2003): SPOT HRV data analysis for detecting earthquake-induced changes in Izmit, Turkey, Int. J. Remote Sens, 24, 2439–2450.

Yonezawa, C., Takeuchi, S. (2001): Decorrelation of SAR data by urban damages caused by the 1995 Hyogoken-nanbu earthquake, International Journal of Remote Sensing, 22(8), 1585–1600.

Yonezawa, C., Tomiyama, N., Takeuchi, S. (2002): Urban damage detection using decorrelation of SAR interferometric data, Geoscience and Remote Sensing Symposium IGARSS '02, 2051–2053.

Yu, S. Z. (2010): Investigation and analysis of earthquake damage to the residential buildings in the Yushu M7.1 earthquake, Journal of Civil, Architectural, and Environmental Engineering, 2(32), 13–15.

Yusuf, Y., Matsuoka, M., Yamazaki, F. (2001): Damage assessment after 2001 Gujarat earthquake using Landsat-7 satellite images, J. Indian Soc. Remote Sens, 29, 17–22.

Prepoznavanje građevina pogođenih potresom temeljem korelacijske detekcije promjena obilježja teksture na SAR snimkama

SAŽETAK. Detekcija oštećenja građevina uzrokovanih potresom od presudne je važnosti za upravljanje rizicima od katastrofa i aktivnostima prilikom elementarnih nepogoda. Metodologije detekcije promjena, koristeći satelitske snimke kao što su podaci radara sa sintetičkim otvorom antene (SAR), korištene su u detekciji oštećenja od potresa. Informacije sadržane unutar SAR podataka, koje se odnose na oštećenja građevina uzrokovana potresom, mogu lako sadržavati šumove zbog drugih faktora. Ovaj rad prikazuje viševremenski pristup detekciji promjena kako bi se identificirale i procijenile informacije koje se odnose na oštećenja od potresa koristeći u potpunosti značajke teksture SAR snimaka. Pristup se temelji na dvije snimke koje su izrađene kroz glavne komponente višestrukih osobina tekstura. Neovisna analiza glavnih komponenti koristi se kako bi se izdvojile komponente višestrukih tekstura. Nakon toga provodi se korelacijska analiza kako bi se detektirale informacije o distribuciji građevina oštećenih potresom. Učinkovitost ove tehnike ispitana je u gradu Jiegu (kojega je 2010. godine pogodio potres Yushu) te u dolini Kathmandu (koju je 2015. godine pogodio potres Nepal), u kojoj je ukupna točnost detektiranja građevina bila 87,8%, odnosno 84,6%. Rezultati međusobne provjere valjanosti pokazali su da je predloženi pristup osjetljiviji od postojećih metoda za detektiranje oštećenih građevina. Općenito govoreći, metoda je učinkovit pristup detektiranja oštećenja koji može u budućnosti pružati potporu u aktivnostima upravljanja nakon potresa.

Ključne riječi: detekcija promjena, radar sa sintetičkim otvorom antene, potres, korelacijska analiza, analiza glavnih komponenti, obilježje teksture.

Received / *Primljeno:* 2017-09-30

Accepted / *Prihvaćeno:* 2018-06-14